High-Gain Wideband Dielectric Resonator Antenna Based on Semi-Cylindrical Grooved Structure

Daotong Li, *Senior Member, IEEE*, Linsong Shi, Jiaxin Wang, *Graduate Student Member, IEEE*, Ying Liu, and Qiang Chen, *Senior Member, IEEE*

***Abstract*—A high-gain wideband cylindrical dielectric resonator antenna (CDRA) based on semi-cylindrical grooved structure is presented in this brief. A semi-cylindrical grooved structure is used to combine the higher-order $HEM_{12\sigma}$ mode of the CDRA with that of the slot resonant mode, so to realize a hybrid radiation mode with high gain characteristics. For further improving the realized gain of the antenna, a pair of parasitic metal panels is employed symmetrically without increasing the horizontal size and profile. Moreover, by employing the $HEM_{12\sigma}$ mode and slot modes concurrently, the proposed high-gain wideband CDRA fed by microstrip-to-stripline feeding structure realizes the wide bandwidth of 5.92GHz. Furthermore, by taking advantage of the bottom of the feed structure, which plays the role of a reflector, the realized gain is improved without requiring further design improvements. Finally, a prototype of demonstration is designed, fabricated and measured. The proposed antenna achieves a peak gain of 12.9dBi over a fractional bandwidth (FBW) of 22.1% around 27 GHz. The measured results agree well with simulated ones. It is a good candidate for 5G millimeter wave wireless communications.**

***Index Terms*—Dielectric resonator antenna, high gain, mm-wave, hybrid modes, wideband, wireless communication.**

I. Introduction

DIELECTRIC resonator antenna (DRA) has the advantages of high design degree of freedom and no metals loss, as well as multiple resonant modes, small size and wideband, which can meet the requirements of B5G/6G applications [1], [2], [3]. Moreover, because the transmission and propagation losses of millimeter wave antenna in free space are relatively severe, the characteristics of high gain wideband DRA are urgent desired.

To enhance the realized gain of DRA, different methods have been proposed [4], [5], [6], [7], [8], [9], [10], [11], [12], [13]. Firstly, the antenna array is adopted to improve the gain [4], [5], and the gains of 9.8 and 17.2dBi are achieved in 1×4 [4] and 4×4 antenna array [5], respectively. Although the gain of antenna can be enhanced by using the array configurations, the overall size of antenna increases. Moreover, the gains of antennas can also be improved by using higher order resonant modes. In [6], the HEM_{133} and HEM_{123} modes are utilized, and the maximum gain of the DRA is 11.6dBi. Nevertheless, its bandwidth is less than 6%. In addition, the hybrid DRA can also be used to improve the antenna gain. The reported antenna in [7] consisting of a CDRA and a truncated plastic conical horn has achieved a peak gain of 11.3dBi with low sidelobe level. However, a high antenna profile of $1.29\lambda_0$ (λ_0 is the wavelength in free space at the center frequency of working frequency band) is achieved due to the addition of plastic horn. Additionally, a CDRA with top-mount spherical cap lens and a metal reflector obtains a fractional bandwidth (FBW) of 65% and a peak gain greater than 14 dBi, which has been proposed in [8] recently. The improvement of its gain performance mainly depends on the functions of lens and reflector. A pattern reconfigurable high gain spherical DRA with three switching modes to control the radiation pattern and the maximum gain of 9.12dBi is achieved in [9], but the bandwidth of 1.7% should be enhanced because of the excitation of higher order TE_{301} mode. A two-layer higher-order-mode circularly polarized (CP) rectangular dielectric resonator antenna (DRA) is proposed in [10], which achieved the CP bandwidth of 9.5% and the maximum gain of 11dBic, while two-layer DRA is difficult to be processed and assembled, and the accuracy requirements of millimeter wave frequency band for DRA is hard to be achieved by using 3D printing technology. A wideband filtering dielectric resonator antenna is proposed in [11], which achieved bandwidth of 34% and the maximum gain of 9.5dBi. But the high profile ($0.55\lambda_0$) and complex circuitry limit its application. DRAs with horn-lens structure are proposed in [12] and [13] to achieve the maximum gains of 19dBi and 13.1dBi, and the bandwidths are 122% and 92.4%, respectively. Both antennas exhibit remarkable EM performance establishing a new state of the art in the area of dielectric antennas. However, the size and profile introduced by the horn, lens and reflector preclude their use in low profile applications.

In this brief, a novel high-gain wideband cylindrical dielectric resonator antenna (CDRA) based on semi-cylindrical

Manuscript received 12 September 2023; revised 1 October 2023; accepted 16 October 2023. Date of publication 23 October 2023; date of current version 5 March 2024. This work was supported in part by the National Natural Science Foundation of China under Grant 61801059; in part by the FY2021 JSPS Postdoctoral Fellowship for Research in Japan under Grant P21053; in part by the Grant-in-Aid for JSPS Research Fellow under Grant 21F21053; in part by the Chongqing University Large Instruments and Equipment Function Development Project under Grant gnkf2023009 and Grant K202016; and in part by the Basic Research and Frontier Exploration Special of Chongqing Natural Science Foundation under Grant cstc2019jcyj-msxmX0350. This brief was recommended by Associate Editor K.-F. Tong. *(Corresponding authors: Daotong Li; Ying Liu.)*

Daotong Li is with the Center of Aerocraft TT&C and Communication and School of Microelectronics and Communication Engineering, Chongqing University, Chongqing 400044, China, and also with Department of Communications Engineering, Tohoku University, Sendai 980-8579, Japan (e-mail: dli@cqu.edu.cn).

Linsong Shi, Jiaxin Wang, and Ying Liu are with the School of Microelectronics and Communication Engineering, Chongqing University, Chongqing 400044, China (e-mail: liuyingcqu@cqu.edu.cn).

Qiang Chen is with the Department of Communications Engineering, Tohoku University, Sendai 980-8579, Japan (e-mail: qiang.chen.a5@tohoku.ac.jp).

Color versions of one or more figures in this article are available at https://doi.org/10.1109/TCSII.2023.3326480.

Digital Object Identifier 10.1109/TCSII.2023.3326480

grooved structure is proposed. It consists of the proposed semi-cylindrical grooved CDRA, the coupling structure and microstrip-to-strip line transition. The working mechanism of the proposed semi-cylindrical grooved CDRA is first analyzed theoretically and numerically. Different from the approaches of multi-layer dielectric combination structure, the high gain performance of proposed CDRA can be achieved by simply adjusting the parameters of semi-cylindrical grooved CDRA. Furthermore, a pair of parasitic metal panels and stripline feeding structure are utilized to improve the gain of the proposed cylindrical grooved CDRA. Eventually, the proposed cylindrical grooved CDRA can obtain a peak gain of up to 13.2dBi, a wide −10dB impedance bandwidth of 5.92 GHz, and compact size of $1.71\lambda_0\times1.33\lambda_0\times0.29\lambda_0$. A prototype is designed, fabricated and measured, with a good agreement between the measured and simulated results. The proposed semi-cylindrical grooved CDRA is a good candidate for 5G millimeter wave communication applications.

II. Antenna Design and Investigation

The structure of the proposed novel high-gain wideband CDRA is shown in *Fig*. 1, which consists of semi-cylindrical grooved CDRA, ground, a pair of parasitic metal panels, coupling structure, feeding substrate and microstrip-to-strip line transition. The 92% alumina ceramic semi-cylindrical grooved CDRA with a high relative permittivity $\varepsilon_r = 8.8$ is located on the center of the feeding substrate. The feeding substrate is Teflon with the relative permittivity $\varepsilon_r = 3.3$, a thickness $t = 0.6$mm and loss tangent $tan\delta = 0.002$. The microstrip-to-strip line transition structure is employed to feed and excite the resonant mode of CDRA through the coupling slot structure. The coupling aperture equals to a magnetic dipole, which provides a fairly good impedance matching for the $HEM_{11\sigma}$ mode in [14].

For the conventional CDRA (Antenna I), if the relative permittivity ε_r maintains a constant, the ratio of r/h will determine the resonant frequency of $HEM_{11\sigma}$ mode, where, r, h, and ε_r are the radius, the height, and the relative permittivity of the CDRA, respectively. Adjusting the r/h ratio can change the resonant frequency and excite the HEM mode. When $r = 3.2$mm, $h = 1.505$mm and the $\varepsilon_r = 8.8$ of the CDRA are determined, the eigenmode resonant frequency of $HEM_{11\sigma}$ mode at 25.2 GHz can be obtained, as shown in Fig. 1(c). It should be mentioned that the maximum gain of the CDRA (Antenna I) based on $HEM_{11\sigma}$ mode is only 6.6dBi due to the excitation of fundamental mode, the radiation pattern can be seen from Fig. 2.

In order to improve the realized gain of CDRA, the higher order mode of CDRA with corresponding feeding structure is a good solution. Higher order mode is usually excited by stacking multiple DRAs or combining several substrates with different relative permittivity. Nevertheless, the stacked multiple DRAs structure inevitably increases the profile, and it is also not convenient to adjust the effective relative permittivity of multilayer substrates. In fact, the excitation of higher order mode can be achieved by controlling only the r/h ratio of CDRA under the slot coupling feed network in [15]. Herein, the semi-cylindrical grooved CDRA (Antenna II) with controllable relative permittivity and aspect ratio is proposed, by combining the semi-cylindrical groove with relative permittivity $\varepsilon_{air} = 1$ and DRA with relative permittivity $\varepsilon_r = 8.8$, an

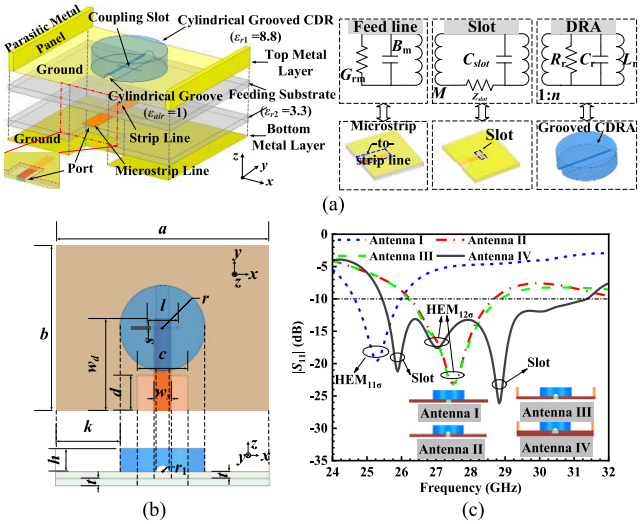

Fig. 1. Geometry of the proposed semi-cylindrical grooved CDRA: a=18mm, b=14mm, c=4.3mm, d=3mm, r=3.6mm, l=2.6mm, s=0.2mm, wd=7.8mm, ws=1.5mm, r_1=0.55mm, h=1.905mm, t=0.6mm, k=5.4mm, (a) 3D view and equivalent circuit model diagram of proposed CDRA, (b) Top view and side view. (c) Evolution and simulated S_{11} of the proposed antenna.

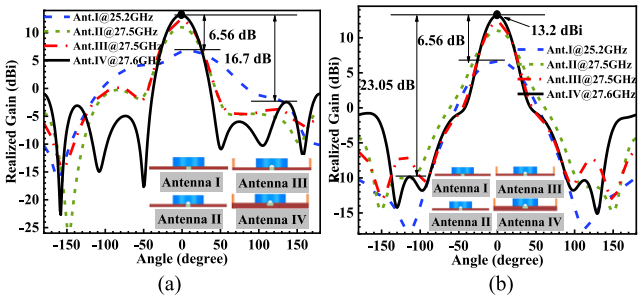

Fig. 2. Realized gain of proposed antenna, (a) E-Plane phi=0°. (b) H-Plane phi=90°.

effective relative permittivity ε_{eff} of CDRA can be derived as:

$$\varepsilon_{\text{eff}} = \frac{V_1\varepsilon_r + V_2\varepsilon_{\text{air}}}{V_1 + V_2} \tag{1}$$

$$V_1 = \pi r^2 h - \pi {r_1}^2 r \tag{2}$$

$$V_2 = \pi {r_1}^2 r \tag{3}$$

where, V_1 and V_2 are the volumes of alumina ceramic dielectric and air dielectric, respectively. R=3.6mm is the radius of the whole CDRA, r_1=0.55mm is the radius of the semi-cylindrical groove, h=1.905mm is the height of the CDRA, ε_r is the relative permittivity of the dielectric resonator, ε_{air} is the relative permittivity of the air and the finally relative permittivity is ε_{eff} =8.46.

The higher order mode $HEM_{12\sigma}$ of CDRA is achieved by a semi-cylindrical grooved CDRA through slot-fed and adjusting the dielectric constants ratio of alumina ceramic CDRA to cylindrical grooved air dielectric, without adding any other dielectric materials and increasing profiles. The coupling coefficient of the slot depends on the aperture size and impedance matching network. The aspect ratio r/h and radius r_1 of the semi-cylindrical grooved structure determines the excitation of the modes. Generally, the change of r/h ratio will affect the resonant mode and the resonant frequency of CDRA, it is worth mentioning that the resonant frequency of

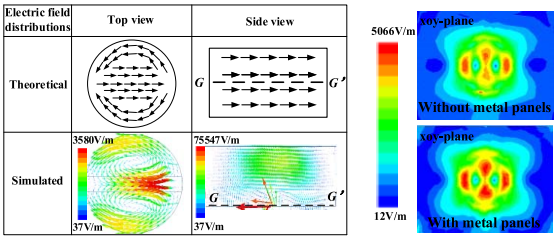

(a) (b)

Fig. 3. (a) Theoretical and simulated electric field vector distributions of $HEM_{12\sigma}$ mode at 27.5GHz. (G-G' is the location of the ground plane) (b) Electric field distributions of CDRA with/without metal panels at 27.5GHz.

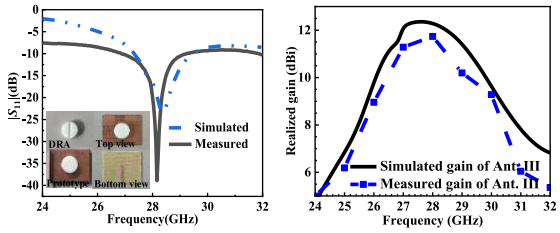

(a) (b)

Fig. 4. Simulated and measured S_{11} and realized gains of the Antenna III. (a) S_{11}, (b) Realized gain.

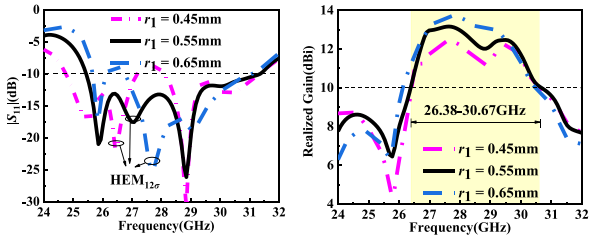

(a) (b)

Fig. 5. Simulated (a) reflection coefficients, and (b) realized gains of the CDRA with different radius r_1 of semi-cylindrical grooved structure.

the proposed CDRA is controlled by changing the relative dielectric constant without affecting the resonant mode of the antenna through the semi-cylindrical grooved structure, as well as the aspect ratio *r*/*h*. As shown in Fig. 1(c), when *r*/*h*=1.88, the radius r_1=0.55mm, the higher order mode $HEM_{12\sigma}$ of Antenna II can be excited at 27.5GHz.

Moreover, Fig. 3(a) shows the comparison of the simulated electric field diagrams of the proposed CDRA and the theoretical electric field diagrams of higher order mode $HEM_{12\sigma}$ at 27.5 GHz. It can be seen that the simulated fields are not completely consistent with the theoretical ones for the proposed CDRA placed on a metal ground plane, because the metal sheet underneath the CDRA changes the boundary conditions. Notably, it also can be determined from the field distributions and gain performance of DRA [16], [17]. From Fig. 3(a), it can be seen that the overall distribution of the electric field vector is similar to the theoretical $HEM_{12\sigma}$ mode in the top and side views. The strong current at the bottom of the antenna in side view is mainly caused by the strong electric field near the slot boundary. Moreover, the distribution of the electric field consists of two electric field loops from the top view, which is consistent with the electric field distribution of eigenmode. Furthermore, the gain of the CDRA (Antenna II) at 27.5GHz achieved 11dBi in Fig. 2, which is same as the gain characteristics of higher order mode. Thus, it can be determined that the $HEM_{12\sigma}$ higher order mode has been excited. Ultimately, the grooved CDRA achieves the maximum gain of 11dBi within band of 26.2-28.5GHz, which are shown in Fig. 1(c) and 2.

Furthermore, to improve the gain of the CDRA (Antenna III), a pair of parasitic metal panels are introduced on both sides of the radiator to constrain the electric field in the *xoy* plane. As shown in Fig. 3(b), it is obvious that the electric field distributions of the CDRA are more concentrated along the direction of the $+z$-axis at the center of the proposed CDRA with parasitic metal panels. In order to verify the high gain characteristic of the antenna with higher order mode, Antenna III is fabricated and measured. As shown in Fig. 4(a), the measured reflection coefficient of the proposed Antenna III is better than –10 dB over 26.6-28.9 GHz (simulated: 26.2-28.8 GHz), which covers the 28 GHz band for the future 5G applications. It is verifiable that the measured result is basically consistent with the simulated one. The gain of the Antenna III prototype in the impedance bandwidth has been shown in Fig. 4(b). The measured maximum gain of Antenna III is 11.6dBi (simulated 12.3dBi), which verifies the high gain performance introduced by the higher order mode.

Although the CDRA with higher order mode $HEM_{12\sigma}$ can improve the gain, the FBW of the CDRA is only 9.4%. Therefore, in order to broaden the working bandwidth and further improve the gain, the slot resonant modes are excited simultaneously by employing the stripline feeding network structure, and a novel wideband high-gain CDRA is proposed, labeled as Antenna IV. As shown in Fig. 1(c), multiple modes of CDRA and slot can be excited by utilizing the microstrip-to-strip line feeding structure and semi-cylindrical grooved structure. Owing to the enclosed construction, the stripline structure extremely reduces the insertion loss during the transmission, especially beneficial for mm-wave applications. In addition, the metal ground of stripline structure also acts as a reflector to further improve the gain performance of the CDRA. Benefiting from the hybrid radiation mode combined by the excitation of slot and DRA, the gain of the CDRA is increased from 12.2dBi to 13.2dBi, and the FBW is improved from 9.4% (26.2-28.8GHz) to 20.8%(25.44-31.36GHz), which can be seen from Fig. 1(c) and 2.

III. Parameters Analysis

In order to gain further insight into the working mechanism of the proposed CDRA, the impacts of some key parameters are investigated theoretically and numerically.

The resonant frequency and impedance bandwidth of the DRA are mainly determined by the size of the resonator. Fig. 5(a) and (b) show the impacts of the radius r_1 of the semi-cylindrical groove on the antenna gain and bandwidth, respectively. As the radius of groove r_1 increases, the effective relative permittivity of the whole CDRA decreases, and the resonant frequency will shift upwards to high frequency. Moreover, the radius r_1 also determines the contact area between the CDRA and the slot, which affect the coupling coefficient of the antenna and the gain performance. As shown in Fig. 5(b), when the resonant frequency of CDRA moves towards to the radiation resonant frequency of slot,

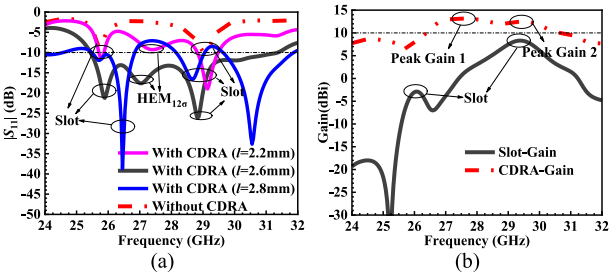

Fig. 6. Simulated S_{11} and gain of the proposed antenna with/without CDRA and impacts of different slot length l on reflection coefficients of the proposed CDRA. (a) reflection coefficients, (b) realized gains.

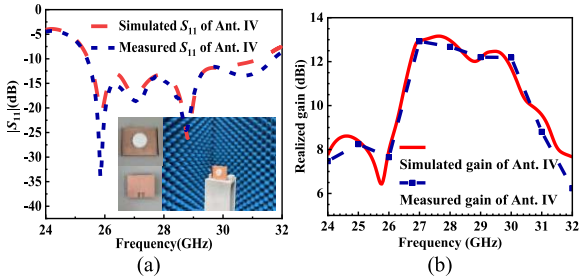

Fig. 7. Simulated and measured S_{11} and realized gain of the proposed antenna. (a) S_{11}, (b) Realized gain.

the maximum gain of the proposed antenna increases. Thus, the gain can be improved by adjusting radius r_1 of the semi-cylindrical groove. Noting that, the resonant frequency of CDRA is too close to or merged with the resonant frequency of slot, which will reduce the bandwidth of the antenna.

For further understanding the working mechanism of proposed antenna with multi-modes, the introduction of additional resonant frequencies 25.9GHz and 28.8GHz were confirmed by removing the CDRA structure and feeding the slot directly as shown in Fig. 6(a). When there is no CDRA resonant mode, there are two potential resonant frequencies in the bandwidth, which are introduced by slot. As shown in Fig. 6(b), the slot not only feeds the DRA but also has the characteristic of radiation, i.e., hybrid radiation modes of both the DRA and the slot contribute to the radiative process. Antenna IV has two peak gain points, one is located around 27GHz mainly achieved by the $HEM_{12\sigma}$ mode of CDRA, and the second peak gain point is around 29.5GHz. It can be seen from Fig. 6(b) that the peak gain point 2 in Antenna IV is at a similar frequency of slot peak gain, which proves the high gain characteristics realized by the combination of CDRA and the radiation of the slot.

As mentioned in Section II, the proposed CDRA is fed by slot coupling, and the coupling coefficient and impedance of the slot are associated with the slot length *l*. The equivalent circuit model of slot coupled DRA is shown in Fig. 1(a), the proposed semi-cylindrical grooved CDRA is modeled as a parallel *RLC* resonator with lumped elements R_r, C_r and L_r. Equivalent capacitance C_{slot} is related with the size of slot, and the coupling between the slot and dielectric radiator is modeled by the transformer with ratio of 1: *n*. The magnitude of fed energy could be controlled with *n* value, which is related with the size of feeding slot. Fig. 6(a) shows the input impedance of the CDRA for different slot length *l*. As the slot length *l* increases from 2.2 to 3mm, the coupling coefficient of the antenna will rise, and the return loss of the working frequency will thus be affected.

IV. Prototype and Results

A. Antenna Prototype

To verify the proposed high gain wideband CDRA fed with the microstrip-to-strip line feeding structure, the Antenna IV is fabricated and measured. The prototype of the proposed CDRA is fabricated by using computer numerical control (CNC) and printed circuit board (PCB) manufacturing. The CDRA is made of 92% alumina ceramic with the relative permittivity ε_r =8.8, and the dielectric substrate is made of RISHO CS-3376C (Teflon) with the relative permittivity ε_r =3.3, a thickness of t = 0.6mm, and $tan\delta$ = 0.002. Fig. 7(a) shows the photographs of the proposed prototype. The antenna is attached to the dielectric substrate by a low relative permittivity adhesive (3M PR100).

B. Measured and Simulated Results

The simulated results were achieved by using ANSYS HFSS (2018) software. For the Antenna IV, the measured -10dB impedance bandwidth is 25.40-31.71GHz (simulated: 25.44-31.36GHz) as shown in Fig. 7(a). There are three resonant frequencies in the working bandwidth, which are consistent with the simulation. Compared with Antenna III, the FBW of Antenna IV has been greatly improved from 8.3% to 22.1% (−3dB gain bandwidth of 14.7%), which verifies the benefit of introducing the microstrip-to-strip line feed structure. Moreover, the measured/simulated maximum gain of Antenna IV in the bandwidth is 12.9/13.2dBi, as illustrated in Fig. 7(b). Due to the no surface wave loss characteristics of the CDRA, the simulated radiation efficiencies of both antennas in the bandwidth are greater than 90%. In order to confirm the stability of the radiation pattern in the bandwidth. The measured and simulated radiation pattern of the Antenna IV in the *xoz* plane (φ=0°) and *yoz* plane (φ=90°) at 25.44 GHz, 27.62 GHz and 31.36 GHz are shown in Fig. 8. It can be clearly seen that the radiation patterns are stable in the whole bandwidth range. Besides, the difference between the main polarization and the cross-polarization level of the radiation pattern at 27.62GHz is −45.3dB (simulated −47.6dB). However, the deviation of the main lobe is caused by the SMK connector, which covers DC-40GHz range. The deviations between the simulation and measurement S-parameter are mainly due to the CDRA and the dielectric substrate are connected by glue and fabrication tolerance.

The performance comparisons between the proposed CDRA and recently reported DRAs research are listed in Table I. The proposed CDRA has the advantages of compact size, wide-band, high gain, simple and easy fabrication which does not require the stacked multilayer dielectric or combination with high profile lens structure. It is worth noting that the proposed semi-cylindrical grooved CDRA can achieve high gain by only adjusting the radius parameters of semi-cylindrical groove, which not increase the antenna's profile. Moreover, the antenna gain is enhanced by increasing the effective radiation aperture due to the pair of metal panels, which does not increase the antenna size, thus achieving miniaturization.

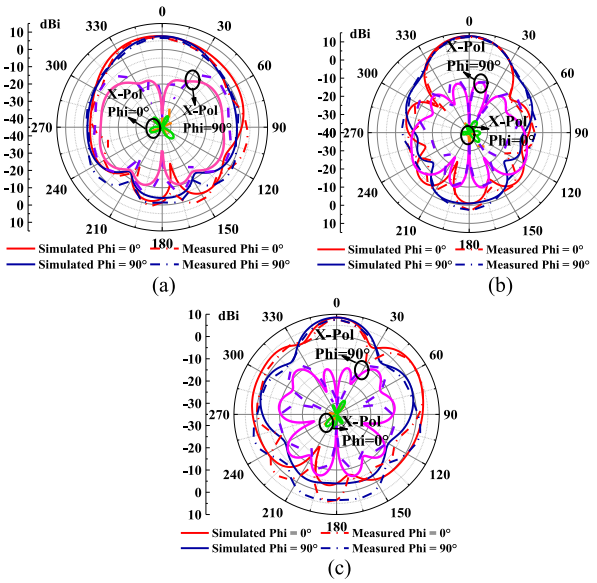

Fig. 8. Simulated and measured radiation patterns of the Antenna IV: (a) 25.44GHz, (b) 27.62GHz, (c) 31.36GHz. (X-pol: — Simulated, --- Measured).

TABLE I
THE PERFORMANCE OF THE PROPOSED ANTENNA WITH THOSE AVAILABLE IN THE LITERATURE

Refs.	Freq. (GHz)	FBW (%)	Design Methods	Resonant Modes	Max Gain (dBi)	Size(λ_0^3)
[6]	5.725-5.875	6	CDRA	HEM_{133}, HEM_{123}	11.59	2.56×2.56×0.47
[7]	27.7-32.7	13.6	CDRA+Horn	$HEM_{111+\sigma}$	12.6	2×2×1.29
[18]	20.1-28.5	34.6	CDRA+SIW	$HEM_{11\sigma}$, $HEM_{12\sigma+1}$	8.15	1.1×1.1×0.12
[19]	7.46-7.84 9.41-11.03	4.98 12.68	HDRA+CDRA	TE_{111}, $TE_{40\sigma}$, $TE_{12\sigma}$	11.72 11.50	3.34×3.34×2.35
[20]	3.24-4	21	RDRA+Groove	TE_{111}	9.6	NA
This Work	**25.40-31.71**	**22.1**	**CDRA+Groove**	**$HEM_{12\sigma}$, Slot**	**12.9**	**1.71×1.33×0.29**

V. CONCLUSION

In this brief, a novel structure of a high-gain, broadband millimeter-wave CDRA is proposed based on semi-cylindrical grooved structure for millimeter wave communications. The characteristics of the proposed semi-cylindrical grooved CDRA are first analyzed. Different from the other works, the proposed antenna simply adopts the semi-cylindrical grooved structure to reach the hybrid radiation modes, and the hybrid modes of the CDRA are realized by combining the $HEM_{12\sigma}$ mode of the CDRA and the resonant mode of slot. Moreover, the working mechanism of the proposed antenna is further investigated theoretically and numerically. Two CDRA prototypes are designed, fabricated, assembled and measured. The result indicates that the proposed antenna achieves the maximum gain of 12.9dBi and the FBW of 22.1%, and a good agreement between simulation and measurement is obtained, which can be used for 5G millimeter wave communications.

REFERENCES

[1] S. Chaudhuri, M. Mishra, R. S. Kshetrimayum, R. K. Sonkar, H. Chel, and V. K. Singh, "Rectangular DRA array for 24 GHzISM-band applications," *IEEE Antennas Wireless Propag. Lett.*, vol. 19, no. 9, pp. 1501–1505, Sep. 2020.

[2] W. Wang and Y. Zheng, "Wideband gain enhancement of a dual-polarized MIMO vehicular antenna," *IEEE Trans. Veh. Technol.*, vol. 70, no. 8, pp. 7897–7907, Aug. 2021.

[3] D. Guha, P. Gupta, and C. Kumar, "Dualband cylindrical dielectric resonator antenna employing $HEM_{11\delta}$ and $HEM_{12\delta}$ modes excited by new composite aperture," *IEEE Trans. Antennas Propag.*, vol. 63, no. 1, pp. 433–438, Jan. 2015.

[4] Y.-T. Liu, B. Ma, S. Huang, S. Wang, Z. J. Hou, and W. Wu, "Wideband low-profile connected rectangular ring dielectric resonator antenna array for millimeter-wave applications," *IEEE Trans. Antennas Propag.*, vol. 71, no. 1, pp. 999–1004, Jan. 2023.

[5] Z. Chen et al., "Millimeter-wave rectangular dielectric resonator antenna array with enlarged DRA dimensions, wideband capability, and high-gain performance," *IEEE Trans. Antennas Propag.*, vol. 68, no. 4, pp. 3271–3276, Apr. 2020.

[6] M. Mrnka and Z. Raida, "Enhanced-gain dielectric resonator antenna based on the combination of higher-order modes," *IEEE Antennas Wireless Propag. Lett.*, vol. 15, pp. 710–713, 2016.

[7] E. Baldazzi et al., "A high-gain dielectric resonator antenna with plastic-based conical horn for millimeter-wave applications," *IEEE Antennas Wireless Propag. Lett.*, vol. 19, no. 6, pp. 949–953, Jun. 2020.

[8] R. Cicchetti, A. Faraone, E. Miozzi, R. Ravanelli, and O. Testa, "A high-gain mushroom-shaped dielectric resonator antenna for wideband wireless applications," *IEEE Trans. Antennas Propag.*, vol. 64, no. 7, pp. 2848–2861, Jul. 2016.

[9] B. K. Ahn, H.-W. Jo, J.-S. Yoo, J.-W. Yu, and H. L. Lee, "Pattern reconfigurable high gain spherical dielectric resonator antenna operating on higher order mode," *IEEE Antennas Wireless Propag. Lett.*, vol. 18, no. 1, pp. 128–132, Jan. 2019.

[10] A. A. Abdulmajid, Y. Khalil, and S. Khamas, "Higher-order-mode circularly polarized two-layer rectangular dielectric resonator antenna," *IEEE Antennas Wireless Propag. Lett.*, vol. 17, no. 6, pp. 1114–1117, Jun. 2018.

[11] H. Liu, H. Tian, L. Liu, and L. Feng, "Co-design of wideband filtering dielectric resonator antenna with high gain," *IEEE Trans. Circuits Syst. II Exp. Briefs*, vol. 69, no. 3, pp. 1064–1068, Mar. 2022.

[12] R. Cicchetti, V. Cicchetti, A. Faraone, L. Foged, and O. Testa, "A wide-band high-gain dielectric horn-lens antenna for wireless communications and UWB applications," *IEEE Trans. Antennas Propag.*, vol. 71, no. 2, pp. 1304–1318, Feb. 2023.

[13] D. Caratelli, R. Cicchetti, V. Cicchetti, and O. Testa, "A wideband high-gain circularly-polarized dielectric horn antenna equipped with Lamé-Axicon stacked-disk lens for remote sensing, air traffic control and satellite communications," *IEEE Access*, vol. 11, pp. 20912–20922, 2023.

[14] R. K. Mongia and P. Bhartia, "Dielectric resonator antennas—A review and general design relations for resonant frequency and bandwidth" *Int. J. Microw. Millimeter-Wave Comput. Aided Eng.*, vol. 4, no. 3, pp. 230–247, Jul. 1994.

[15] A. K. Ojha and A. V. Praveen Kumar, "High gain broadside mode operation of a cylindrical dielectric resonator antenna using simple slot excitation" *Int. J. Microw. Wireless Techn.*, vol. 13, no. 3, pp. 286–294, APR. 2021.

[16] D. Guha, A. Banerjee, C. Kumar, and Y. M. M. Antar, "Higher order mode excitation for high-gain broadside radiation from cylindrical dielectric resonator antennas," *IEEE Trans. Antennas Propag.*, vol. 60, no. 1, pp. 71–77, Jan. 2012.

[17] A. W. Glisson, D. Kajfez, and J. James, "Evaluation of modes in dielectric resonators using a surface integral equation formulation," *IEEE Trans. Microw. Theory Techn.*, vol. 31, no. 12, pp. 1023–1029, Dec. 1983.

[18] M.-D. Yang, Y.-M. Pan, Y.-X. Sun, and K.-W. Leung, "Wideband circularly polarized substrate-integrated embedded dielectric resonator antenna for millimeter-wave applications," *IEEE Trans. Antennas Propag.*, vol. 68, no. 2, pp. 1145–1150, Feb. 2020.

[19] S. Varghese, P. Abdulla, A. M. Baby, and P. M. Jasmine, "High-gain dual-band waveguide-fed dielectric resonator antenna," *IEEE Antennas Wireless Propag. Lett.*, vol. 21, no. 2, pp. 232–236, Feb. 2022.

[20] S. Fakhte, H. Oraizi, and L. Matekovits, "Gain Improvement of rectangular dielectric resonator antenna by engraving grooves on its side walls," *IEEE Antennas Wireless Propag. Lett.*, vol. 16, pp. 2167–2170, 2017.